EUROPEAN JOURNAL OF COMPUTATIONAL MECHANICS, 2016
VOL. 25, NO. 6, 446–474
http://dx.doi.org/10.1080/17797179.2016.1253364

Taylor & Francis
Taylor & Francis Group

Spectrally formulated user-defined element in conventional finite element environment for wave motion analysis in 2-D composite structures

Ashkan Khalili[a], Ratneshwar Jha[a] and Dulip Samaratunga[b]

[a]Department of Aerospace Engineering, Mississippi State University, Starkville, MS, USA; [b]Space Materials Laboratory, The Aerospace Corporation, El Segundo, CA, USA

ABSTRACT

Wave propagation analysis in 2-D composite structures is performed efficiently and accurately through the formulation of a User-Defined Element (UEL) based on the wavelet spectral finite element (WSFE) method. The WSFE method is based on the first-order shear deformation theory which yields accurate results for wave motion at high frequencies. The 2-D WSFE model is highly efficient computationally and provides a direct relationship between system input and output in the frequency domain. The UEL is formulated and implemented in Abaqus (commercial finite element software) for wave propagation analysis in 2-D composite structures with complexities. Frequency domain formulation of WSFE leads to complex valued parameters, which are decoupled into real and imaginary parts and presented to Abaqus as real values. The final solution is obtained by forming a complex value using the real number solutions given by Abaqus. Five numerical examples are presented in this article, namely undamaged plate, impacted plate, plate with ply drop, folded plate and plate with stiffener. Wave motions predicted by the developed UEL correlate very well with Abaqus simulations. The results also show that the UEL largely retains computational efficiency of the WSFE method and extends its ability to model complex features.

ARTICLE HISTORY
Received 22 August 2016
Accepted 14 October 2016

KEYWORDS
Wavelet spectral finite element; user-defined element; wave propagation; structural health monitoring; composite structures

1. Introduction

Wave propagation in elastic structures has significance for several applications such as nondestructive evaluation (NDE), transient response prediction and mechanical property characterisation (Graff, 1975; Rose, 2004). Among these, NDE is perhaps the most common application as ultrasonic waves are often used for inspection of engineering structures. Advanced composites have several advantages compared to metallic materials such as higher specific strength and

CONTACT Ratneshwar Jha Jha@ae.msstate.edu

modulus, fewer joints, improved fatigue life and higher resistance to corrosion leading to their growing use in aerospace, wind energy and civil infrastructure. Much research has recently been carried out on NDE of composites using Lamb waves due to several advantages it offers over existing methods (Chimenti, 1997; Nayfeh, 1995). Lamb waves are elastic waves that are generated in a solid plate with free boundaries and are also known as plate waves. Lamb waves are able to travel long distances with little dispersion allowing rapid scan of large areas. These features of Lamb waves coupled with the ease of application with integrated actuators and sensors has enabled *in situ* damage diagnosis also known as structural health monitoring (SHM). SHM is nondestructive evaluation through integrated actuators and sensors and has been a very active area of research in the past decade. A lot of work has been carried out over the last decade contributing to the development of Lamb wave-based SHM (Boller, Chang, & Fujino, 2009; Diamanti & Soutis, 2010; Giurgiutiu, 2007; Raghavan & Cesnik, 2007; Su, Ye, & Lu, 2006). However, there are many challenges yet to be addressed before this method is implemented practically. Computational modelling is essential for complete understanding of Lamb wave propagation in composite structures. Physics-based models for wave propagation may also be used for generating baseline data which is necessary in ultrasonic inspection systems.

Modelling of wave propagation in composite structures is much more complex compared to the isotropic structures (Rose, 2004; Nayfeh, 1995). It is very difficult to obtain the governing differential equations and boundary/initial conditions for wave propagation in most practical structures. Numerical methods are often used, which include the conventional finite element method (FEM) (Lee & Staszewski, 2003; Ochoa & Reddy, 1992; Talbot & Przemieniecki, 1975), finite difference method (Graves, 1996; Strikwerda, 2004), pseudospectral method (Fornberg, 1987) and boundary element method (Beskos, 1997). FEM is the most popular numerical technique for wave motion analysis. However, 20 nodes are generally needed spanning a wavelength for accurate predictions (Ochoa & Reddy, 1992), which makes FEM-based wave propagation analysis at high frequencies very expensive computationally. Spectral finite element (SFE), based on the transformation of wave equations into the frequency domain, is highly suitable for wave propagation analysis (Doyle, 2012; Gopalakrishnan, Chakraborty, & Mahapatra, 2008; Gopalakrishnan & Mitra, 2010). SFE requires only one element to model a beam or plate structure of any length if there are no discontinuities. Just a few elements can model wave motion in a simplified practical structure such as a stiffened plate, leading to very high computational efficiency.

Use of an integral transform method, which transforms variables between frequency and time domains, is a key component in SFE implementation. Doyle (2012) popularised the fast Fourier transform (FFT)-based spectral finite element (FSFE) to model wave motion in isotropic 1-D and 2-D waveguides. Mitra and Gopalakrishnan (2008) presented the 2-D wavelet based spectral

finite element (WSFE) to overcome some limitations of FSFE and accurately model 2-D plate structures of finite dimensions. WSFE uses orthogonal compactly supported Daubechies scaling functions (Daubechies, 1992) as the basis for both temporal and spatial approximations. Jha and associates developed WSFE based on the first-order shear deformation theory (FSDT) which was a major improvement compared to the previously reported classical laminated plate theory based models (Samaratunga, Jha, & Gopalakrishnan, 2014a). The developed WSFE was validated with Abaqus FEM simulations using shear flexible elements. Excellent correlation was observed in the results and WSFE computation time was less than two orders of magnitude compared to Abaqus (Samaratunga et al., 2014a). Composite plates with transverse cracks were also modelled using WSFE (coded in Matlab) and validated with Abaqus FEM simulations (Samaratunga, Jha, & Gopalakrishnan, 2014b). WSFE models with additional complexity such as adhesively bonded joints and skin stiffener structures have also been developed by the authors (Samaratunga, Jha, & Gopalakrishnan, 2014c, 2016). Thus, WSFE is well established for regularly shaped structures like rod, beam and plate. However, modelling complex structural features (holes, cut-outs, etc.) and damages (impact, delamination, crack, etc.) with spectral finite element method presents difficulties. These limitations stem from the difficulty in deriving governing equations and boundary conditions for modelling structures with complex features. Assembling spectral elements of different types and dimensions would give us the ability to model complex structures and damages while retaining the computational efficiency of WSFE. The present authors earlier reported UEL formulation for thick beams (Khalili, Samaratunga, Jha, & Gopalakrishnan, 2014; Khalili, Samaratunga, Jha, Lacy, & Gopalakrishnan, 2015).

In the present work, we develop WSFE-based User Elements (UEL) that can be implemented in conventional finite element platform to analyse ultrasonic wave propagation in 2-D composite structures accurately and efficiently. The new user element is implemented in commercial finite element code Abaqus through UEL subroutine. One of the major aspects of this research is that all of the variables in WSFE have complex value in the frequency domain. For UEL implementation in Abaqus, a complex value is represented as a 2×2 matrix of real numbers which leads to doubling the number of degrees of freedom. All of the structures in numerical examples are modelled and meshed using Abaqus CAE and WSFE formulation-based elements are assigned as element type using UEL. The numerical examples include five different cases, namely, healthy plate, plate with impact damage, plate with ply drop, folded plate and plate with stiffener. This approach provides access to powerful modelling tools, pre- and post-processing, and efficient solvers of Abaqus along with the computational efficiency of the WSFE method.

The subsequent sections contain a summary of WSFE plate element formulation, details of UEL development, validation of results through comparison with Abaqus simulations and concluding remarks.

2. WSFE formulation for a composite plate

A summary of the WSFE formulation for a composite plate is presented here; interested readers are referred to (Samaratunga et al., 2014a) for further details. Consider a laminated composite plate of thickness h with the origin of the global coordinate system located at the mid-plane of the plate with Z axis being normal to the mid-plane as shown in Figure 1(a) and (b) shows the corresponding nodal representation of the spectral element. Using FSDT, the governing equations for wave propagation involve the five degrees of freedom (DOFs) at each node: u, v, w, ϕ and ψ (Khalili et al., 2015). The terms $u(x, y, t)$ and $v(x, y, t)$ are mid-plane ($z = 0$) displacements along X and Y axes; $w(x, y, t)$ is transverse displacement in Z direction, and $\psi(x, y, t)$ and $\phi(x, y, t)$ are the rotational displacements about Y and X axes, respectively. The displacements w, ϕ and ψ do not change along the thickness (Z direction). The quantities (N_{xx}, N_{xy}, N_{yy}) are in-plane force resultants, (M_{xx}, M_{xy}, M_{yy}) are moment resultants and (Q_x, Q_y) denote the transverse force.

The governing wave equations are PDEs with respect to two spatial dimensions and time. The WSFE formulation begins with transformation of the field variables (displacements) on to the frequency-wavenumber domain using the scaling functions for Daubechies compactly supported wavelet (Daubechies, 1992). Scaling functions of order 22 are used for temporal approximation and scaling functions of order 4 are used for spatial (lateral dimension) approximation (Samaratunga et al., 2014a), thereby reducing the PDEs to ODEs. Daubechies compactly supported scaling functions have only a finite number of nonzero filter coefficients which enables easy handling of finite geometries and imposition of boundary conditions. Use of wavelet transform has clear advantages in modelling finite wave guides over widely used Fourier transform which has global support basis functions (Mitra & Gopalakrishnan, 2008).

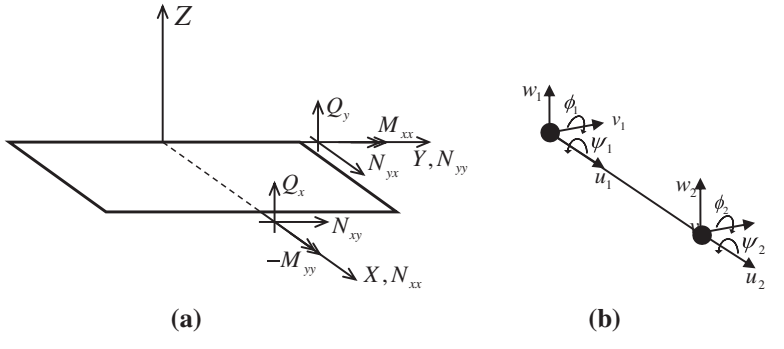

Figure 1. (a) Plate element (b) nodal representation with DOFs.

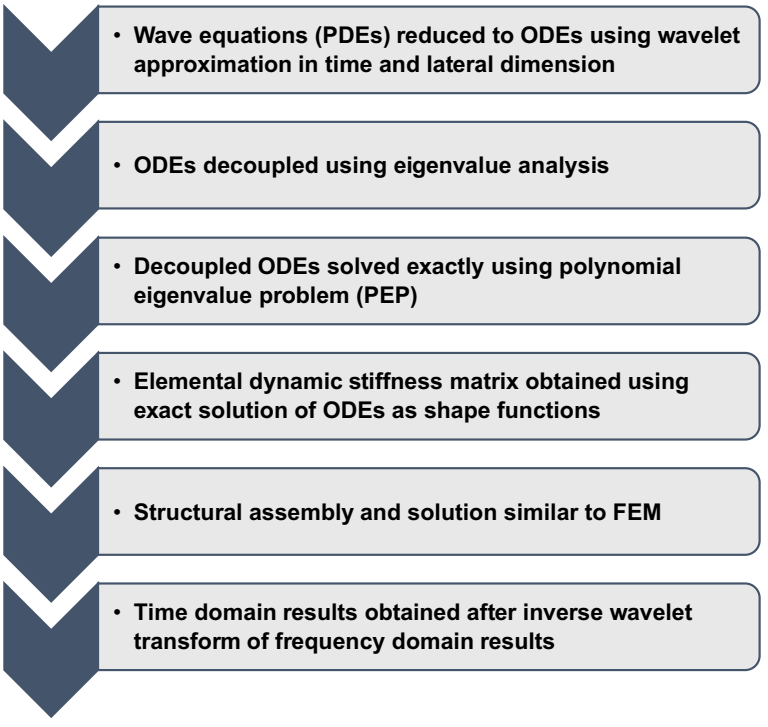

Figure 2. Summary of WSFE procedure for a composite plate.

Time approximated coupled PDEs are decoupled using eigenvalue analysis. Next, the time approximated PDEs are reduced to a set of ODEs using another Daubechies scaling function approximation in lateral spatial (Y) direction. Frequency-dependent wave characteristics corresponding to each lateral wave number are extracted directly from the formulation. The ODEs resulting from spatial approximation are derivatives only of the remaining spatial variable x. The natural boundary conditions are also transformed similarly. The solution of these ODEs to derive the exact shape function involves determination of wave numbers and the amplitude ratio matrix. Unlike isotropic cases, the process of solution for composite materials is more complicated and is done by posing it as polynomial eigenvalue problem (Mitra & Gopalakrishnan, 2008).

Finally, the transformed nodal forces and transformed nodal displacements are related as $\{\tilde{\mathbf{F}}^e\} = [\tilde{\mathbf{K}}^e]\{\tilde{\mathbf{u}}^e\}$ where $[\tilde{\mathbf{K}}^e]$ is the exact elemental dynamic stiffness matrix. Solution of the final equation and the assembly of the elemental stiffness matrices to obtain the global stiffness matrix are similar to the conventional FEM technique. One major difference is that the time integration in FEM uses a suitable finite difference scheme; however, the WSFE performs dynamic stiffness generation, assembly, and solution through a double do-loop over frequency and horizontal wavenumber. Although this procedure is computationally expensive, the problem size in WSF is very small which keeps overall low computational cost. Another difference is that unlike FEM, WSFE deals with only one dynamic

stiffness matrix and hence matrix operation and storage require minimum computations. The decoupled ODEs are solved and the final solutions $u(x, y, t)$, $v(x, y, t)$, $w(x, y, t)$, $\phi(x, y, t)$ and $\psi(x, y, t)$ are obtained using inverse wavelet transform twice for spatial Y dimension and time. Figure 2 presents a summary of the WSFE method.

3. User-defined element based on wavelet spectral finite element

User subroutines in a commercial software give the ability of defining new elements or material properties to expand the capabilities of the software. User-Defined Element (UEL) is a subroutine for defining new elements in Abaqus. Along with the newly defined UEL, the current approach takes advantage of Abaqus modelling capabilities, powerful pre- and post-processing tools, and highly efficient solver. Here we present the details of UEL formulation for 2-D plates.

Determination of elemental stiffness matrix is the most important step in formulating an UEL. Along with the elemental stiffness matrix, two other quantities must be defined as well: right-hand-side vector (residual nodal fluxes or forces) and solution-dependent state variables. Degrees of freedom at each node and the number of nodes in each element are also needed. Figure 3 shows the UEL interface that shows the variables to be defined (RHS, AMATRX, SVARS and ENERGY), variables that can be updated (PNEWDT) and variables passed in for information (rest of the variables) (Dassault Systèmes Simulia Corp, 2014).

Wavelet spectral finite element works in the frequency domain and, thereby, all the parameters such as stiffness matrix, wavenumbers, displacements and forces, have complex values. However, Abaqus computations can use real numbers only. To overcome to this problem, the following mathematical rule is used wherein every complex number can be represented as a 2×2 matrix of real

```
      SUBROUTINE UEL(RHS,AMATRX,SVARS,ENERGY,NDOFEL,NRHS,NSVARS,
     1 PROPS,NPROPS,COORDS,MCRD,NNODE,U,DU,V,A,JTYPE,TIME,DTIME,
     2 KSTEP,KINC,JELEM,PARAMS,NDLOAD,JDLTYP,ADLMAG,PREDEF,NPREDF,
     3 LFLAGS,MLVARX,DDLMAG,MDLOAD,PNEWDT,JPROPS,NJPROP,PERIOD)
C
      INCLUDE 'ABA_PARAM.INC'
C
      DIMENSION RHS(MLVARX,*),AMATRX(NDOFEL,NDOFEL),PROPS(*),
     1 SVARS(*),ENERGY(8),COORDS(MCRD,NNODE),U(NDOFEL),
     2 DU(MLVARX,*),V(NDOFEL),A(NDOFEL),TIME(2),PARAMS(*),
     3 JDLTYP(MDLOAD,*),ADLMAG(MDLOAD,*),DDLMAG(MDLOAD,*),
     4 PREDEF(2,NPREDF,NNODE),LFLAGS(*),JPROPS(*)

      user coding to define RHS, AMATRX, SVARS, ENERGY, and PNEWDT

      RETURN
      END
```

Figure 3. UEL interface which shows all the variables (written in Fortran [Dassault Systèmes Simulia Corp, 2014]).

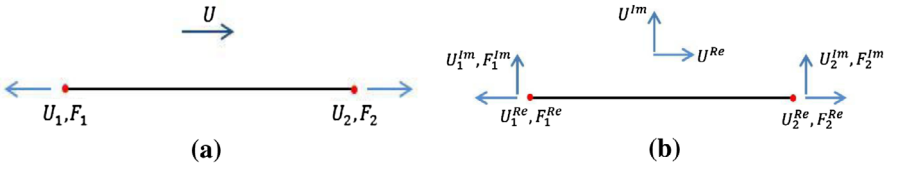

Figure 4. A two-node truss element with (a) complex values; (b) real values.

numbers (Equation 1). A set of complex number forms a field and the matrices of this form are exactly the field of complex numbers. The absolute value of the complex numbers can be calculated as square root of the determinant of the matrix. Further details about matrix representation of complex numbers are explained by Hongbao (2014).

$$a + ib \rightarrow \begin{bmatrix} a & b \\ -b & a \end{bmatrix} \tag{1}$$

Applying this method doubles the dimension of a complex-valued matrix to obtain a matrix with real values, that is, an $n \times n$ matrix with complex values is represented as a $2n \times 2n$ matrix with real values. As an example, consider a rod element with one DOF at each node (Figure 4(a)). The stiffness matrix for this element has the dimension of 2×2. In the frequency domain analysis, all terms in Equation 2 have complex values wherein $K_{11} = K_{11}{}^{Re} + iK_{11}{}^{Im}$ (and similarly for all other terms.)

$$\begin{Bmatrix} F_1 \\ F_2 \end{Bmatrix} = \begin{bmatrix} K_{11} & K_{12} \\ K_{21} & K_{22} \end{bmatrix} \begin{Bmatrix} U_1 \\ U_2 \end{Bmatrix} \tag{2}$$

Applying the matrix representation for complex values doubles the size to obtain a matrix equation with real numbers (Equation 3). Now, this matrix equation can be solved within Abaqus since all terms have real values only.

$$\begin{Bmatrix} F_1^{Re} \\ F_1^{Im} \\ F_2^{Re} \\ F_2^{Im} \end{Bmatrix} = \begin{bmatrix} K_{11}^{Re} & K_{11}^{Im} & K_{12}^{Re} & K_{12}^{Im} \\ -K_{11}^{Im} & K_{11}^{Re} & -K_{12}^{Im} & K_{12}^{Re} \\ K_{21}^{Re} & K_{21}^{Im} & K_{22}^{Re} & K_{22}^{Im} \\ -K_{21}^{Im} & K_{21}^{Re} & -K_{22}^{Im} & K_{22}^{Re} \end{bmatrix} \begin{Bmatrix} U_1^{Re} \\ U_1^{Im} \\ U_2^{Re} \\ U_2^{Im} \end{Bmatrix} \tag{3}$$

The plate element in WSFE (Figure 2) has two nodes and there are five DOFs at each node. To decouple the real and imaginary parts of forces, displacements and stiffness terms, we obtain effectively ten DOFs per node. One can choose to use ten DOFs per node or double the number of nodes (Figure 4) to have five DOFs per node. In this work, we use five DOFs per node and double the number of nodes.

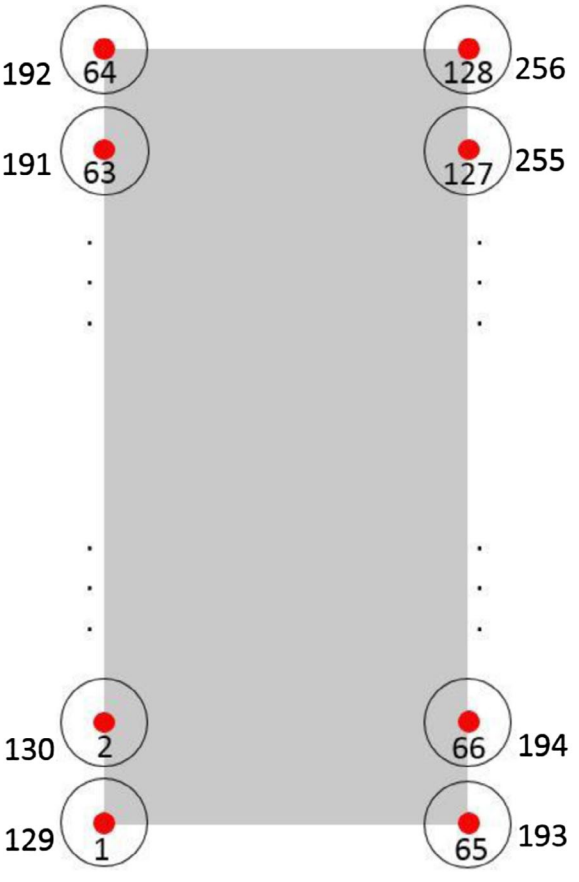

Figure 5. Plate element and nodal representation for UEL based on WSFE.
Notes: Red dots represent real nodes and black circles represent imaginary nodes (co-located with real nodes). Numbers show node numbering in UEL.

Another issue that arises in formulating WSFE-based UEL relates to the discretisation points along the lateral edges. As mentioned previously, each lateral edge is discretised at m points during spatial approximation in WSFE formulation. In order to implement the spatial approximation through UEL, every discretisation point is modelled as two nodes (one each for real and imaginary parts). This leads to $2m$ nodes at each lateral edge and, thus, the plate element has $4m$ nodes with five DOFs at each node (Figure 5). In this research m is chosen as 64. With five DOFs per node, the elemental stiffness matrix has the dimension of 1280×1280. Although the UEL leads to a large elemental stiffness matrix, several measures are implemented for computational efficiency. The eigenvalues and eigenvectors for the frequency-dependent stiffness matrix are calculated only once and stored for subsequent frequency increments. Similarly, stiffness constants and inertial coefficients are calculated just once (first increment) and saved in the solution-dependent state variables (SVARS) array which is accessed throughout the analysis.

The stiffness matrix in global coordinate system is defined as

$$\left[\tilde{K}_G\right] = [T]^T \left[\tilde{K}_e\right][T] \tag{4}$$

where subscript G denotes the values in global coordinate system and e stands for elemental coordinate system. $[T]$ is the transformation matrix and can be written as:

$$[T] = \begin{bmatrix} [Q] & [0] \\ [0] & [Q] \end{bmatrix} \tag{5}$$

$$[Q] = \begin{bmatrix} c & 0 & 0 & 0 & s & 0 & 0 & 0 & 0 & 0 \\ 0 & c & 0 & 0 & 0 & s & 0 & 0 & 0 & 0 \\ 0 & 0 & 1 & 0 & 0 & 0 & 0 & 0 & 0 & 0 \\ 0 & 0 & 0 & 1 & 0 & 0 & 0 & 0 & 0 & 0 \\ -s & 0 & 0 & 0 & c & 0 & 0 & 0 & 0 & 0 \\ 0 & -s & 0 & 0 & 0 & c & 0 & 0 & 0 & 0 \\ 0 & 0 & 0 & 0 & 0 & 0 & 1 & 0 & 0 & 0 \\ 0 & 0 & 0 & 0 & 0 & 0 & 0 & 1 & 0 & 0 \\ 0 & 0 & 0 & 0 & 0 & 0 & 0 & 0 & 1 & 0 \\ 0 & 0 & 0 & 0 & 0 & 0 & 0 & 0 & 0 & 1 \end{bmatrix}$$

The terms c and s denote cosine and sine of the angle between local and global coordinate systems. The transformation matrix (Equation 5) has a dimension of 20×20 due to the decoupling of real and imaginary parts.

It must be noted that in implementing this UEL, Abaqus is used just as a solver without being aware of the physics of the problem. Although the problem is a dynamic one (wave propagation), GENERAL STATIC solver in Abaqus is used for solution. The real and imaginary parts of the solution are combined to obtain results in the frequency domain, and then inverse wavelet transform is used to obtain time domain solutions (Khalili et al., 2014, 2015).

Load distribution along the Y-axis (Figure 2) is given by Equation 6.

$$F(Y) = e^{-(Y/\alpha)^2} \tag{6}$$

where α is a variable to change the distribution of the load long Y-axis. In all of the analysis in this paper, α is selected as 0.05 which causes a Gaussian distribution of load along the edge. The UAMP subroutine is used to define edge load on the element. Load is defined once in the beginning and then saved in a common block to be accessed during rest of the analysis.

An Abaqus subroutine named URDFILL is used to write a code for transformation of results from frequency domain to time domain using inverse wavelet transform. It should be recalled that the results (displacements) are obtained in the frequency domain in WSFE analysis. Obtained results from collocated real and imaginary nodes are coupled to form the frequency domain results as complex numbers. For all of the frequency increments, the results (complex values) are saved in an array and then transformed to the time domain after the last increment for computational efficiency.

4. Numerical experiments

The 2-D WSFE-based user-defined element is used to study axial and transverse wave propagation in composite plates. Computational efficiency and accuracy of the newly developed UEL and its ability to model complex features are also demonstrated. Numerical experiment results are presented in the time domain and compared to FEM results. FEM results are obtained using Abaqus dynamic implicit simulation employing 8-node shell element (S8R5) which is shear flexible and able to model multiple layers. Using shell elements in Abaqus for wave propagation analysis has been reported earlier (Samaratunga et al., 2014a, 2014c, 2016). Hanning windowed sinusoid (tone burst) signal with 3.5 cycles and central frequency of 20 kHz (Figure 6) is used as input load. The spatial domain distribution of load is defined using Equation 6 with $\alpha = 0.05$. AS4/3501-6 graphite-epoxy with material properties mentioned in Table 1 is used for all of the simulations. Models are simulated using a desktop computer with 3.4 GHz Intel Core i7 CPU and 16 GB memory.

Five different cases are simulated and compared with FEM: healthy plate, plate with impact damage, plate with ply drop, plate with stiffener and plate with two

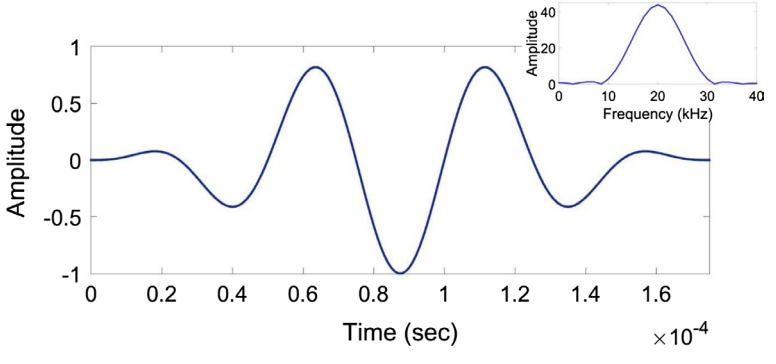

Figure 6. A 3.5 cycle tone burst signal and its frequency content (20 kHz central frequency).

Table 1. Material properties (AS4/3501-6).

E_{11}	144.48*e*9 Pa	E_{33}	9.63*e*9 Pa	G_{13}	4.128*e*9 Pa	υ_{12}	0.02	υ_{23}	0.3
E_{22}	9.63*e*9 Pa	G_{12}	4.128*e*9 Pa	G_{23}	4.128*e*9 Pa	υ_{13}	0.02	Density	1389 kg/m^3

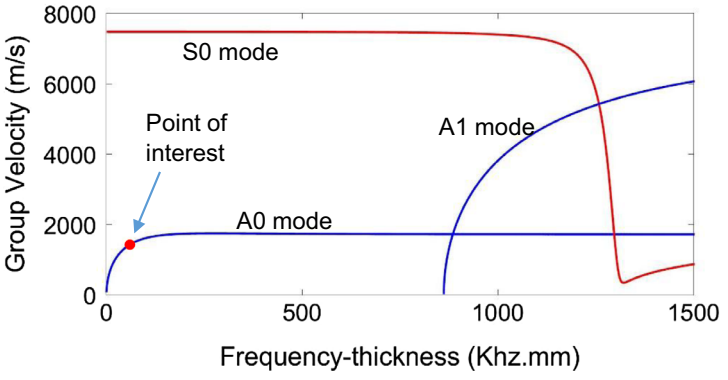

Figure 7. Dispersion curve for AS4/3501 laminate obtained using Disperse software.

folds. Load is always applied at the free edge and simulation results are presented at different points on the plates. Comparison of CPU time and number of elements is given in tables. In all the cases, a symmetric lay up of $[0/90/0/90]_s$ is used except for ply drop example for reasons explained later.

Using Disperse software (Lowe & Pavlakovic, 2013), dispersion curve (group velocity versus frequency-thickness) is obtained as shown in Figure 7. Group velocity for A_0 mode (first asymmetric mode) at 80 kHz-mm is 1537 m/s. In all of the numerical examples, element size in FEM models is chosen based on 20 nodes per wavelength as recommended by Ochoa and Reddy (Ochoa & Reddy, 1992). Wavelength is given by

$$\lambda = \frac{C_g}{f} \tag{7}$$

where C_g is the group velocity and f is the frequency.

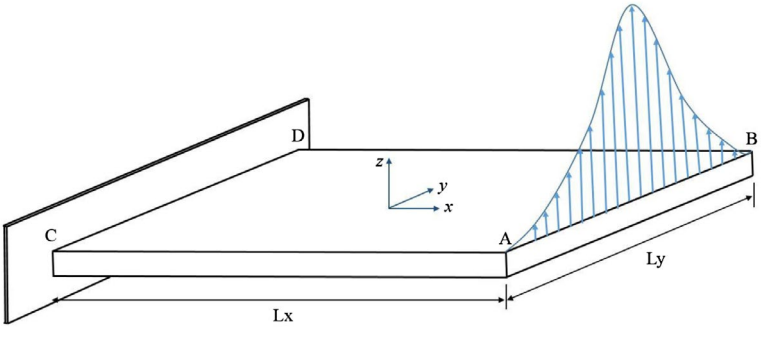

Figure 8. Schematic view of plate.

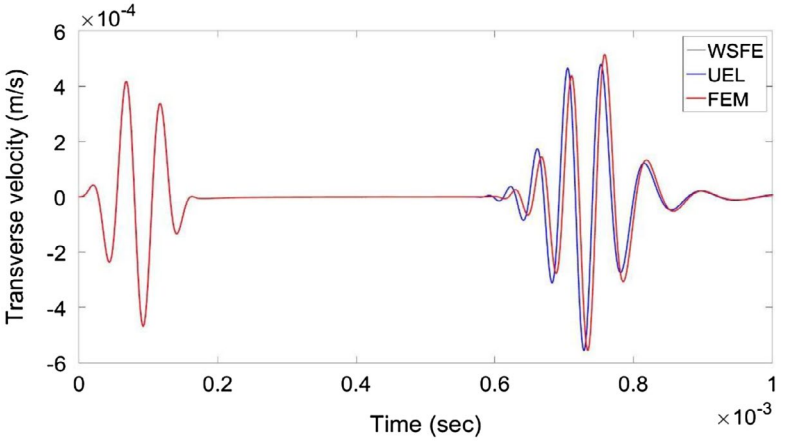

Figure 9. Transverse velocity response of a healthy plate to a tone-burst signal at the tip.

4.1. Healthy plate

4.1.1. Numerical validation

A healthy plate with $[0/90/0/90]_s$ layup in cantilever configuration is modelled using the developed UEL. The plate has dimensions of 0.5 m × 0.5 m and its thickness is 0.004 m. A schematic view of the plate is illustrated in Figure 8. Using UEL, the plate is modelled as a 256-node element with 5 DOFs per node. Resulting elemental stiffness matrix has the dimension of 1280 × 1280.

A 3.5 cycle tone-burst with 20 kHz central frequency is applied at the free edge of the plate (AB) in *Z*-direction. Spatial distribution and point of application of the load (along *Y*-axis) are shown in Figure 8. Wave propagation results are obtained in all three different directions (*X*, *Y* and *Z*) at two different points on the plate: central point of the free edge and mid-point of the plate. For validation purposes, the results are compared to those obtained from two other simulations: WSFE (coded in MATLAB) and Abaqus (FEM).

Hereafter, UEL, FEM and WSFE are used to refer to WSFE-based UEL, FEM model in Abaqus and WSFE method coded in Matlab, respectively. Since there is no discontinuity in the plate, the entire plate can be modelled using just one element in UEL and WSFE models, whereas FEM model contains 10,000 elements. The time domain results for UEL and WSFE are identical so there is no difference visible between them in Figure 9. The incident wave for UEL and FEM match completely and there is a very small difference in the boundary reflections. This difference is likely due to the difference in element formulations between UEL and

Table 2. CPU time comparison – healthy plate.

	Number of elements	Element type	Time (sec)
WSFE	1	WSFE	133
UEL	1	WSFE	726
FEM	10,000	8-noded Shell Elements	6517

Abaqus. As mentioned earlier, UEL is based on the first shear deformation theory while Abaqus model uses S8R5 elements. The group velocity for A_0 mode for the plate lay-up and thickness is 1537 m/s (based on results from Disperse software). Accordingly, the time of flight for a wave to travel from plate tip to the fixed boundary and come back to the tip after reflection should be 0.00065 s. The UEL simulation shows the first reflection from the fixed boundary arriving at 0.00059 s which is very close to the predicted value. Table 2 shows that the computation time for FEM is 6517 s which is almost 10 times higher than the computation time for UEL (726 s). WSFE is the most efficient method computationally since UEL works within a large FE solver (Abaqus).

4.1.2. Experimental validation

Experimental investigation is conducted to validate the accuracy of the results obtained from WSFE and UEL. As discussed earlier (Figure 9), the time domain results for WSFE and UEL are indistinguishable, hence experimental validation figures showing WSFE represent UEL results as well. A composite plate with $[0/90/0/90]_s$ layup is fabricated from AS4/3501-6 pre-preg following vacuum bag technique. The plate has a dimension of 0.42 m × 0.317 m and thickness of 0.0014 m. A piezoelectric (PZT) actuator with 7 mm diameter is bonded to the surface of the composite plate using epoxy adhesive. A National Instruments PXI 6339 and a BNC-2110 board are used to generate a tone burst signal and a QuickPack® power amplifier is used to amplify the actuation signal. In order to investigate the sensitivity of the WSFE to different frequencies, two tone burst excitations (3.5 cycle) with different central frequencies (25 and 50 kHz) are used to generate Lamb waves in the composite plate. A Scanning Laser Vibrometer (SLV) is employed to sense the wave motion at two points, P1 and P2 (shown in Figure 10). Figure 10(a) shows the location of actuator and sensing points whereas experimental set up is illustrated in Figure 10(b).

The acquired velocity data at two sensor points, P1 and P2, are then compared to the results obtained from the WSFE model. Figure 11 shows the comparison between experimental data and the WSFE simulation results for tone burst signal with central frequency of 25 kHz while Figure 12 shows the comparison for 50 kHz excitation frequency.

The experimentally acquired velocity profiles show very good agreement with the WSFE simulation results for all the four cases (two sensor locations and two excitation frequencies). These results demonstrate the capability of WSFE (and UEL) model to accurately predict the wave motion in composite plates even at high frequencies such as 50 kHz.

4.2. Plate with impacted area

Impact damage is a major area of concern for composite structures and Lamb waves have shown a lot of potential for their detection. To study wave motion in a

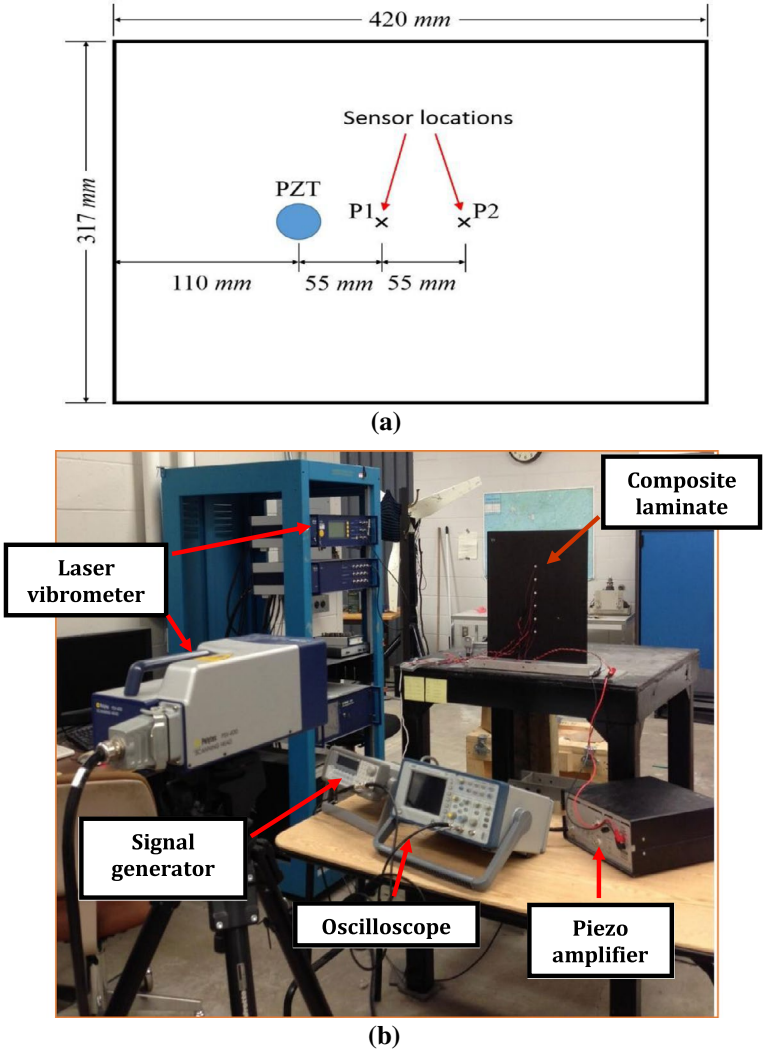

Figure 10. (a) A schematic view of the plate with PZT and sensor locations; (b) experimental set-up.

plate damaged by an impact, the stiffness is reduced by 50% in the impacted area placed in the middle of the plate length. Figure 13 shows a schematic view of the plate which is modelled in fixed-free configuration. The square plate dimensions are 0.4 m along X- and Y- axes, while the location of impacted area is given by $L_1 = L_2 = 0.19$ m and $L_d = 0.02$ m. The thickness of the plate is 0.008 m. Three elements are used to model the plate using UEL while FEM needs 6400 elements to capture the wave propagation accurately.

The 3.5 cycle 20 kHz tone-burst input load is applied on the free edge of the plate in the transverse (Z) direction and results are compared at the two points shown in Figure 13. Figure 14 shows the comparison of time domain results between UEL and FEM at both points. Partial reflections from impacted area are observed

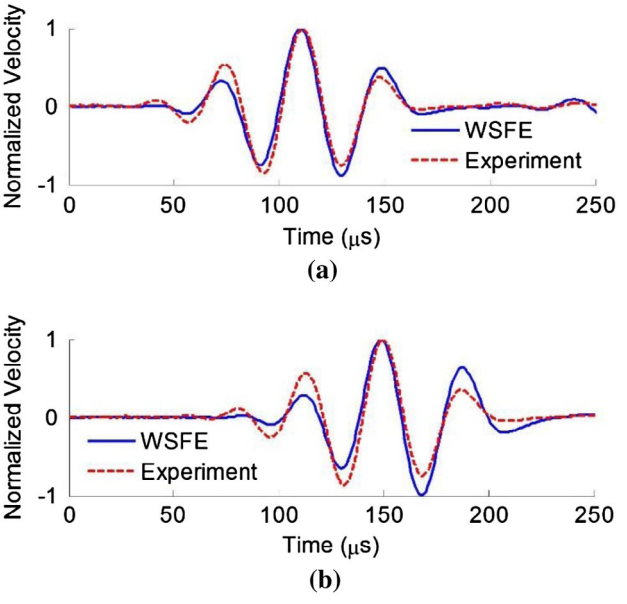

Figure 11. Response comparison for 25 kHz input at (a) P1 and (b) P2.

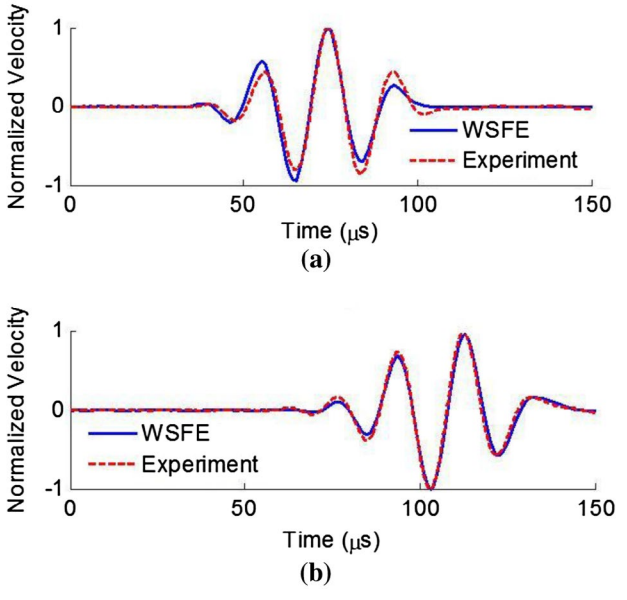

Figure 12. Response comparison for 50 kHz input at (a) P1 and (b) P2.

clearly in both cases. The first wave packet (incident wave) and reflections from the impacted area show excellent match. The fixed boundary reflections show some differences in wave arrival times largely due to differences in element types as noted earlier.

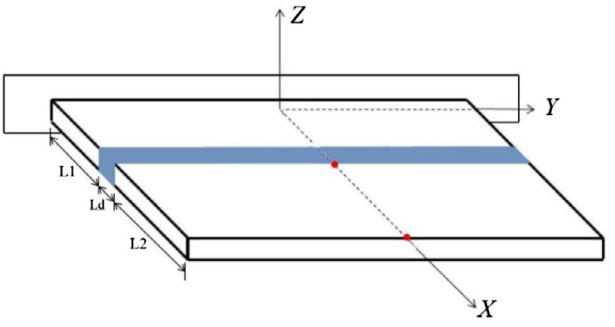

Figure 13. Schematic view of a plate with impacted area is shown in blue.
Note: Red dots show the points where results are obtained.

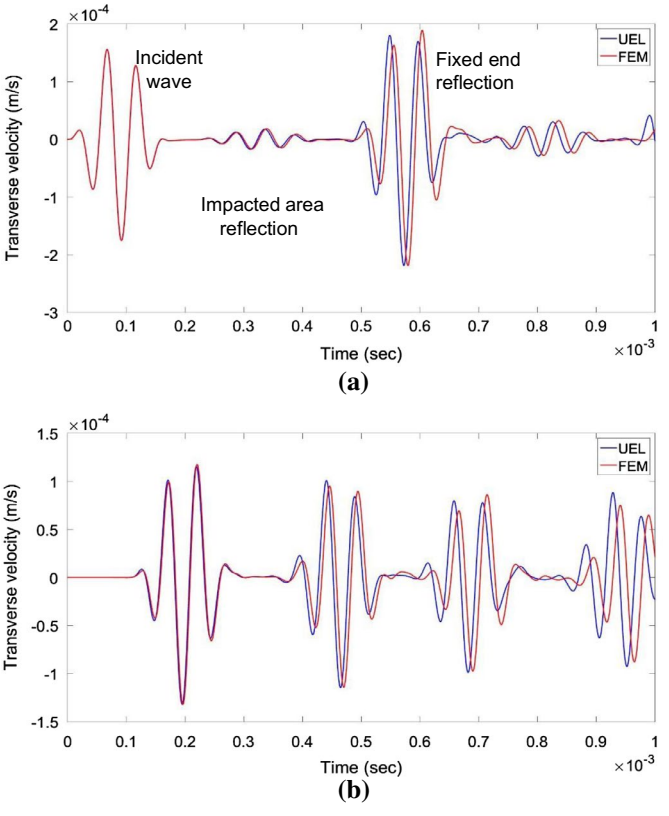

Figure 14. Transverse wave propagation in a plate with impacted area (a) Response at the plate tip, and (b) Response at the midpoint of the impact (right edge).

It is often instructive to visualise the wave propagation in complex structures. Employing dummy elements to define contact surfaces, tie, or visualise while using UEL has been reported in (Salahouelhadj, Abed-Meraim, Chalal, & Balan, 2012) and the same approach is used here to visualise wave propagation in the impacted plate. Dummy elements share the same nodes as UEL and have a

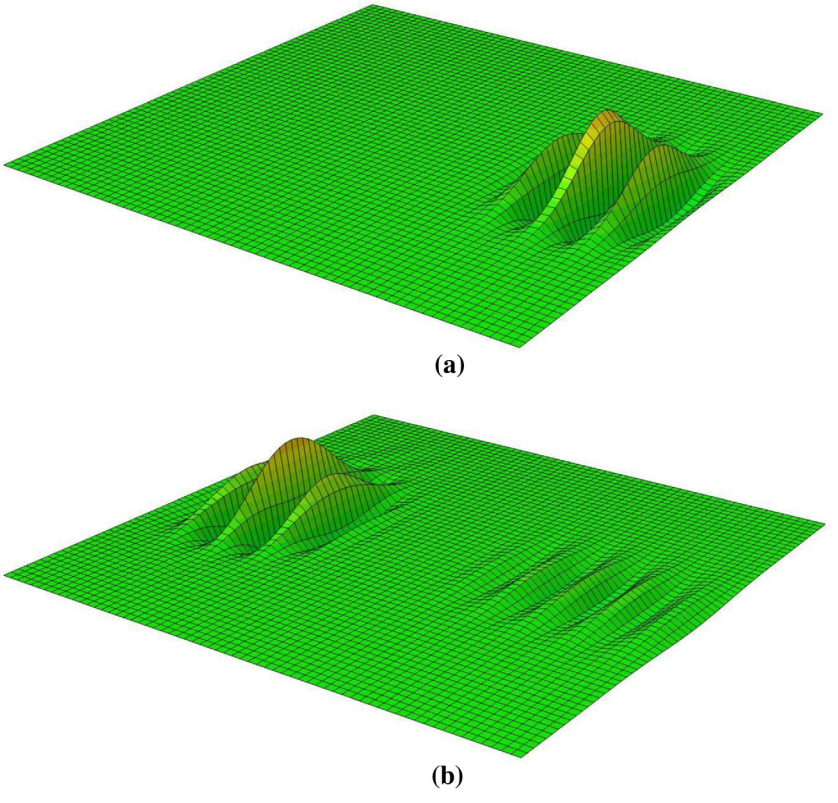

Figure 15. Wave propagation in a $[0/90/0/90]_s$ composite laminate with impacted area in the middle at time instants (a) 80 μs, and (b) 240 μs.
Note: Partial reflection from the impacted area is visible in Figure 15(b).

Table 3. CPU time comparison – impacted plate.

	Number of elements	Element type	Time (sec)
UEL	3	WSFE	1252
FEM	6400	8-noded Shell Elements	3955

negligible stiffness. A python script is written to produce a new output database file to assign the displacements to each node of dummy elements. Figure 15 shows wave propagation in the impacted plate at two different time instances where we clearly observe the incident wave (Figure 15(a)) and the wave reflected from impact region (Figure 15(b)).

A comparison between run time for UEL and FEM simulations is shown in Table 3 along with the number of elements used. The CPU time for UEL is 1252 s while it is 3955 s for FEM, that is, UEL is more than 3 times faster than FEM.

4.3. Plate with ply drops

Ply drop is an essential feature of manufacturing composite structures such as aircraft wings. A 1.5-m long and 0.5-m wide plate with ply drops (Figure 16) is modelled to demonstrate the ability of UEL in simulating such complexities. The plate has eight plies at the root (line GH) and its thickness reduces to 4 plies at the tip (line AB) wherein ply thickness equals 0.001 m. The plate is fixed at the left end (along line GH) and all other edges are free. The 3.5 cycle, 20 kHz tone-burst excitation is applied at the free edge (AB) in the axial (X) direction.

For UEL modelling, the plate is divided into three regions along the X-axis. The first region, from the fixed end to line EF has the layup of $[0/90/0/90]_s$ with a thickness of 0.008 m. The second region, EF to CD has $[90/0/90]_s$ layup and 0.006 m thickness. The last region has $[0/90]_s$ lay-up and 0.004 m thickness. Since there are two discontinuities in the plate (two ply drops), three elements are used in UEL modelling. FEM model needs 30,000 elements for simulating wave motion in this structure.

Figure 17(a) shows axial velocity measured at the plate tip (midpoint of line AB). As expected, two reflections are observed before the fixed end boundary reflection arrives. The ply drops act as discontinuities and the first two reflections are associated with the first and the second ply drops, respectively. For the measurement point located at midpoint of line CD (Figure 17(b)), there is only one reflection observed before the boundary reflection arrives. Results from UEL and FEM show very good match for the incident wave, reflections from first and second ply drops, and fixed end boundary reflection. Significant differences are observed at later time instances where the waves undergo multiple interactions with discontinuities (ply drops and plate boundaries). Table 4 shows the run time comparison between UEL and FEM simulations showing more than 13 times higher computational efficiency for UEL

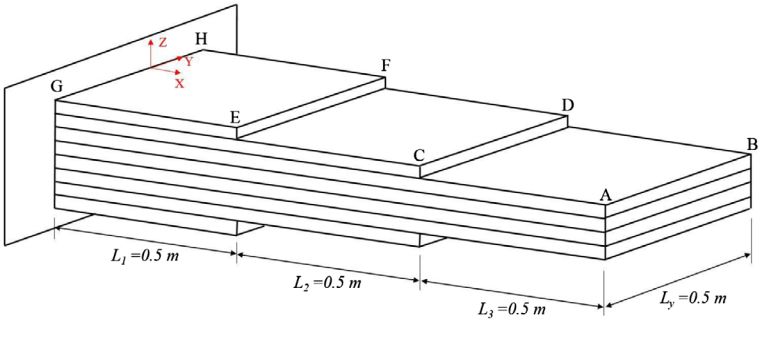

Figure 16. Schematic view of a plate with ply drops.

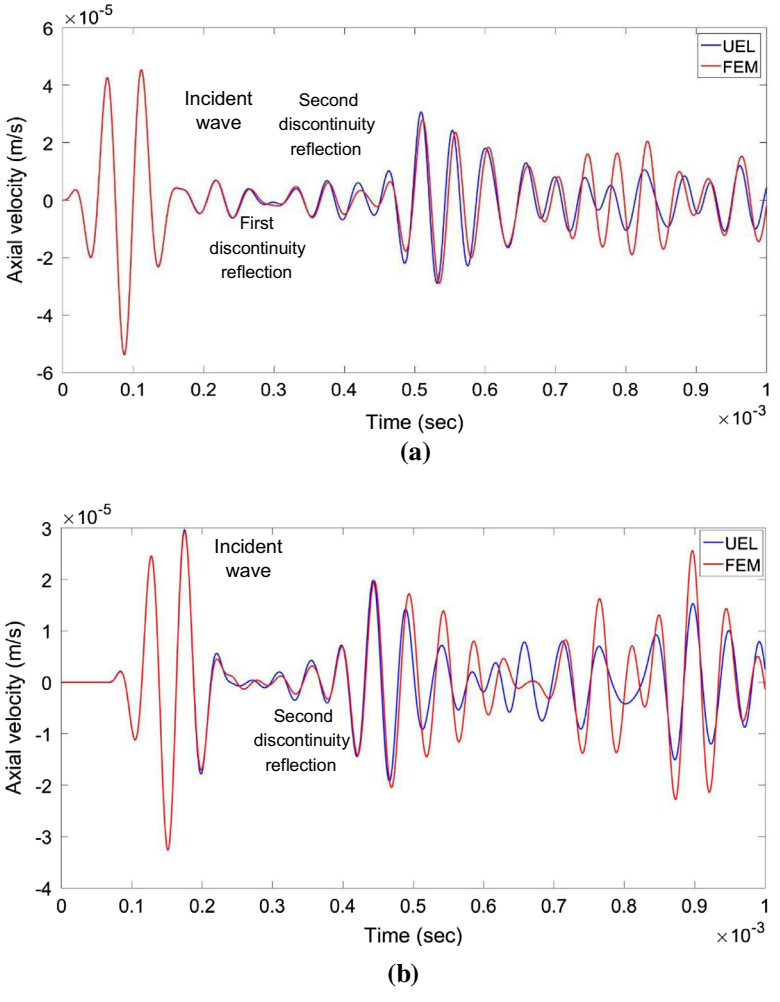

Figure 17. Axial velocity response of a plate with ply drops for two sensing locations: (a) Response at plate tip, and (b) Response at midpoint of line CD.

Table 4. CPU time comparison – plate with ply drops.

	Number of elements	Element type	Time (sec)
UEL	3	WSFE	1252
FEM	30,000	8-noded Shell Elements	16,434

4.4. Folded plate

A folded plate represents a three-dimensional structure wherein waves undergo mode conversions at fold lines (discontinuities). A 1.5-m long and 0.5-m wide plate with two folds is modelled to examine the ability of UEL for simulating structures in 3D space. The entire structure has a symmetric lay-up of $[0/90/0/90]_s$ with 0.008 m thickness. The fold lines divide the structure into three parts (two slanted plates and one main plate) and all three parts have the same dimension

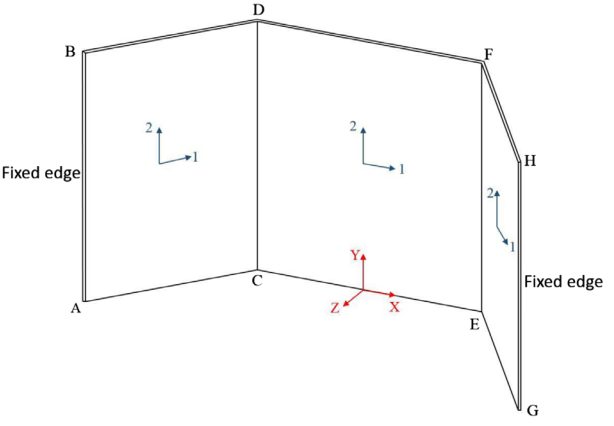

Figure 18. Schematic view of a folded plate.
Note: The coordinate system in red colour (*X*–*Y*–*Z*) indicates global coordinates and the coordinate system associated with each element is shown in blue.

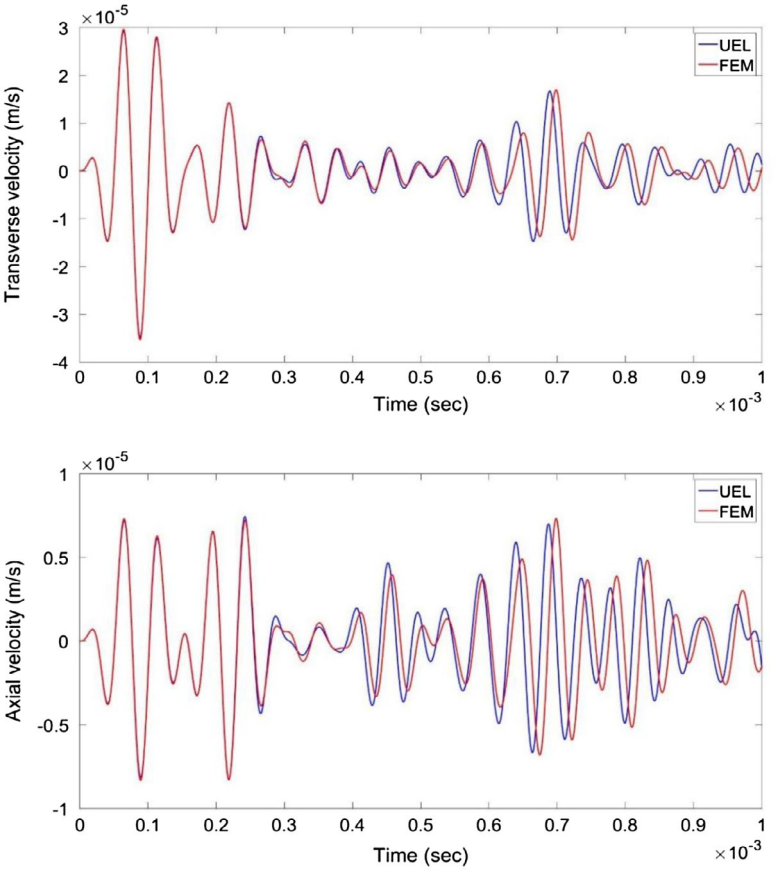

Figure 19. Transverse and axial velocity response of a folded plate to a tone-burst signal.
Note: Responses measured at midpoint of line EF.

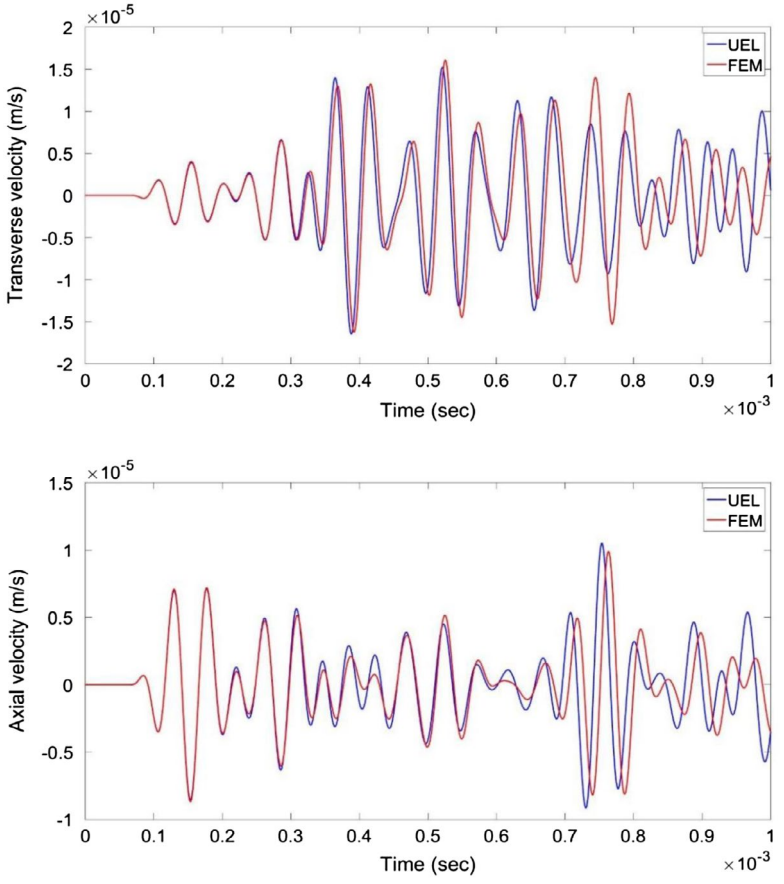

Figure 20. Transverse and axial velocity response of a folded plate to a tone-burst signal.
Note: Responses measured at midpoint of line CD.

of 0.5 m × 0.5 m (Figure 15). The two slanted plates have 45 degree angle with the *X*-axis (rotation about *Y*-axis). In Figure 18, the coordinate system in red colour (*X*–*Y*–*Z*) shows the global coordinate system and the coordinate systems associated with each element are shown in blue. The plate is fixed along AB and GH edges. The 3.5 cycle 20 kHz tone-burst input load is applied at EF edge in *Z*-direction with the spatial distribution given previously in Equation 6.

Since the fold lines act as discontinuities, three elements are used for UEL modelling to represent each region (two slanted plate and one main plate). The three elements are assembled along the local 1-direction. For this purpose, a transformation matrix (Equations 4 and 5) is applied to obtain the stiffness matrix in global coordinate system for each element. The FEM model needs 30,000 elements for the same simulation.

Axial and transverse velocities from UEL and FEM are compared at two locations on the plate (midpoints of edges EF and CD) given in Figures 19 and 20, respectively. The incident waves have perfect match while minor differences are observed in the reflections from the fold lines (discontinuity). The incident wave

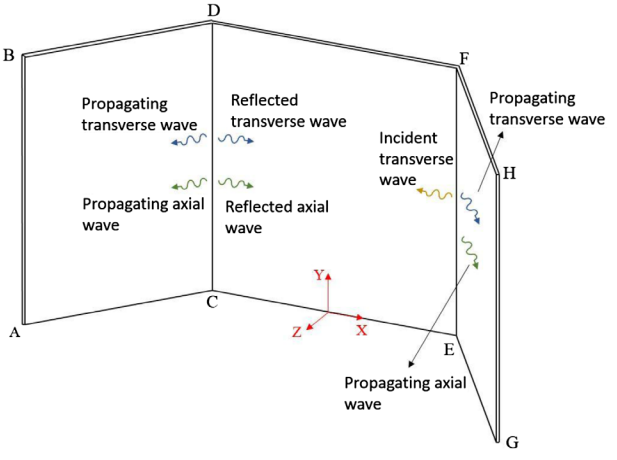

Figure 21. Wave propagation in a folded plate.
Note: Blue arrows represent waves in *Z*-direction (transverse waves) and green ones represent the waves in *X*-direction (axial waves).

Table 5. CPU time comparison – folded plate.

	Number of elements	Element type	Time (sec)
UEL	3	WSFE	947
FEM	30,000	8-noded Shell Elements	17,964

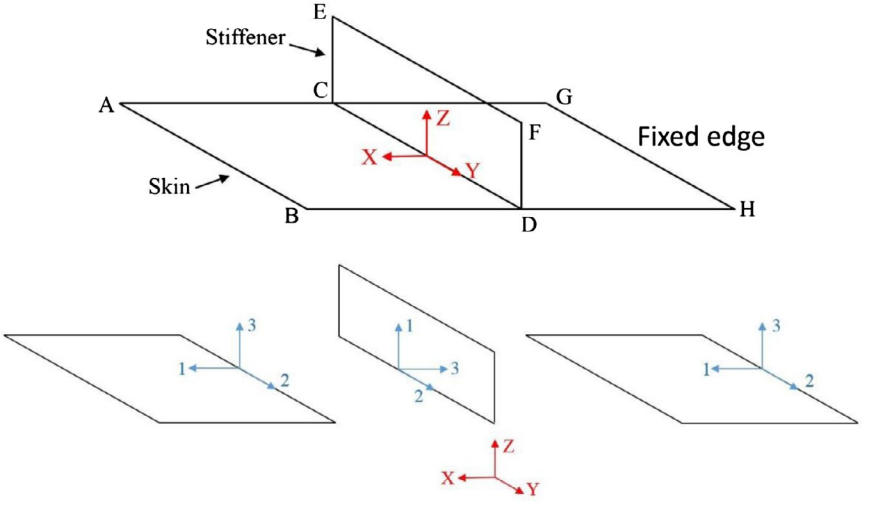

Figure 22. Schematic view of a plate with stiffener.
Note: Global coordinate system (*X*–*Y*–*Z*) is shown in red and the local coordinate systems for each element are shown in blue.

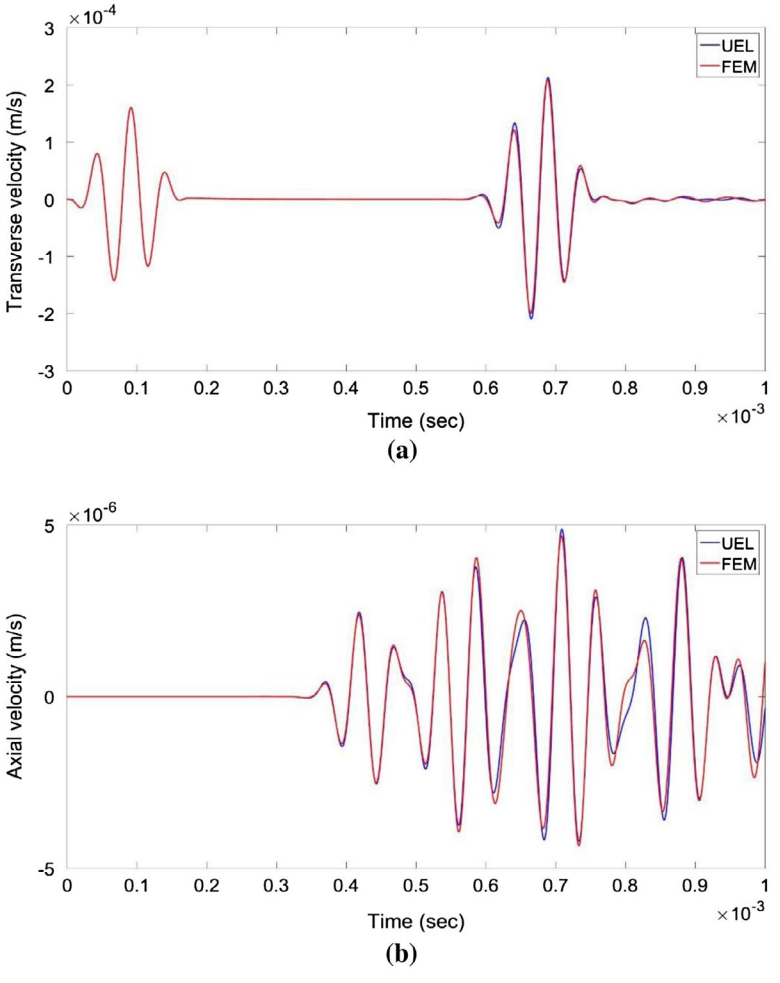

Figure 23. Wave motion in plate with stiffener at midpoint of edge AB: (a) transverse velocity, and (b) axial velocity.

is in Z-direction (transverse), but both axial and transverse waves are observed in the responses. This indicates that a partial wave mode change occurs when the incident transverse wave interacts with the fold lines (Figure 21). Table 5 compares the CPU time and number of elements for UEL and FEM simulations. The run time for UEL is 947 s while the same simulation needs 17,964 s using FEM, thus UEL is almost 20 times faster than FEM.

4.5. Skin-stiffener structure

Stiffened plates are widely used in light weight aerospace structures since they can carry both in-plane and out of plane loadings. Figure 22 illustrates the schematic view of a skin-stiffener structure used to study wave propagation. The entire

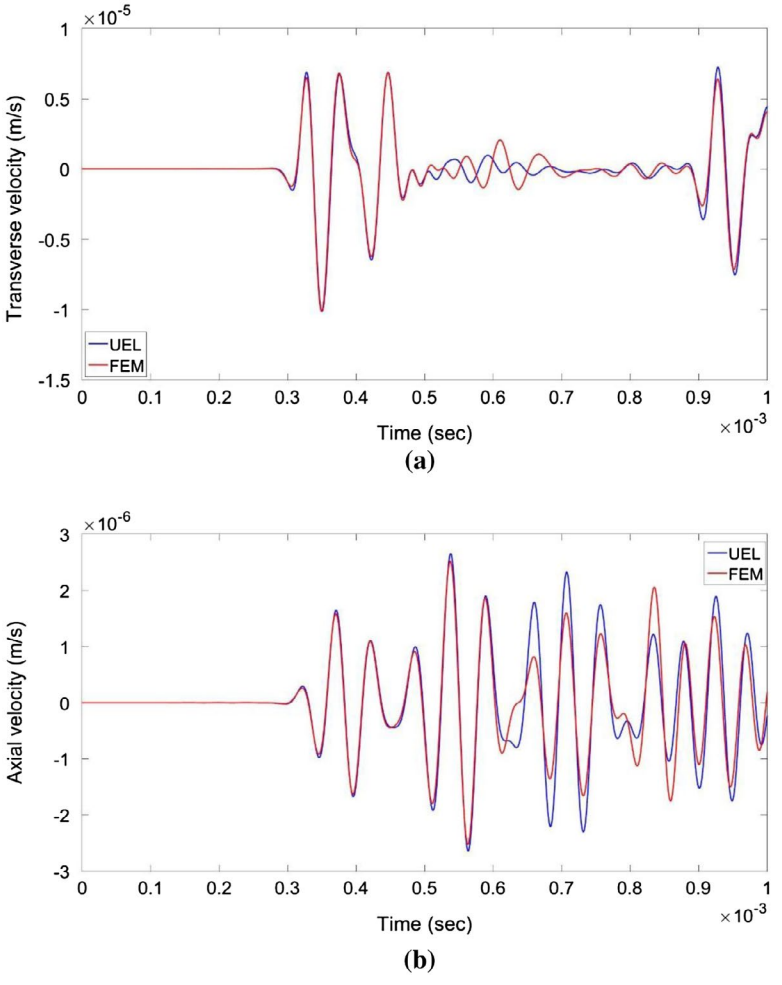

Figure 24. Wave motion in plate with stiffener at midpoint of edge CD: (a) transverse velocity, and (b) axial velocity.

structure can be divided into two regions, skin and stiffener, wherein the stiffener has a 90 degree rotation with respect to skin. In this numerical example, the skin has a dimension of 1 m × 0.5 m while the stiffener dimension is 0.5 m × 0.25 m. Both skin and stiffener have a symmetric lay-up of $[0/90/0/90]_s$ and 0.008 m thickness. The structure is fixed along the edge GH. Load is applied in Z-direction as a 3.5 cycle tone-burst with 20 kHz central frequency acting along the free edge of the skin (AB) with a spatial distribution given in Equation 6.

Three elements are used to simulate wave propagation in the stiffened structure with UEL, two elements to model the skin and one element is used for the stiffener. The two skin elements and the stiffener are assembled along line CD, that is, all three elements share nodes along line CD. Figure 22 also shows the local coordinate system (1–2–3) for each element in blue colour and the global coordinate system (X–Y–Z) is shown in red colour. The transformation matrix

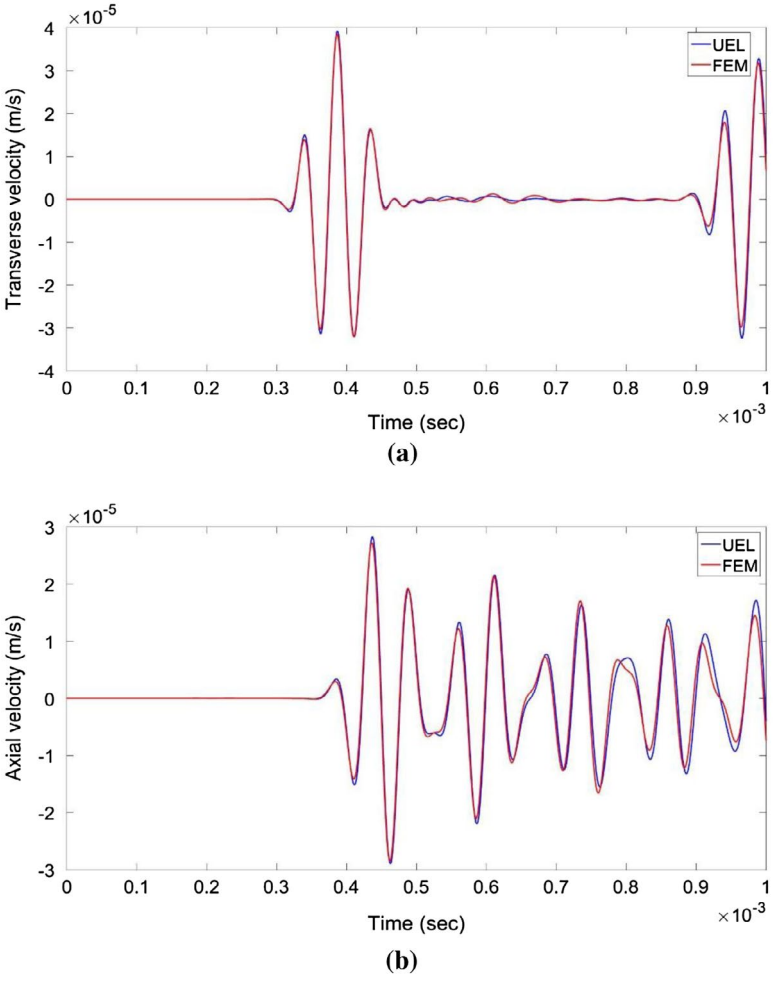

Figure 25. Wave motion in plate with stiffener at midpoint of edge EF: (a) transverse velocity, and (b) axial velocity.

discussed previously (Equation 5) is applied on the elemental stiffness matrices to transform them to the global coordinate system before assembly.

Figure 23 compares time domain results at the midpoint of edge AB showing excellent match between UEL and FEM simulations. It is observed that there is a delay for axial wave arrival at the plate tip. The incident wave is in transverse (Z) direction and initially there is no axial wave till the transverse wave reaches edge CD (stiffener), and then partially reflects back to plate tip after mode conversion. Figures 24 and 25 show similar plots for two other locations, namely the midpoint of edges CD and EF, respectively. Again, there is very good match between UEL and FEM results, including the top of stiffener (line EF). Figures 26(a) and (b) show the wave propagation visualisation in the skin-stiffener structure at two time instants, 120 and 512 μs, respectively. Figure 26(b) clearly shows that most of the incident wave is reflected by the skin-stiffener joint and only a small part

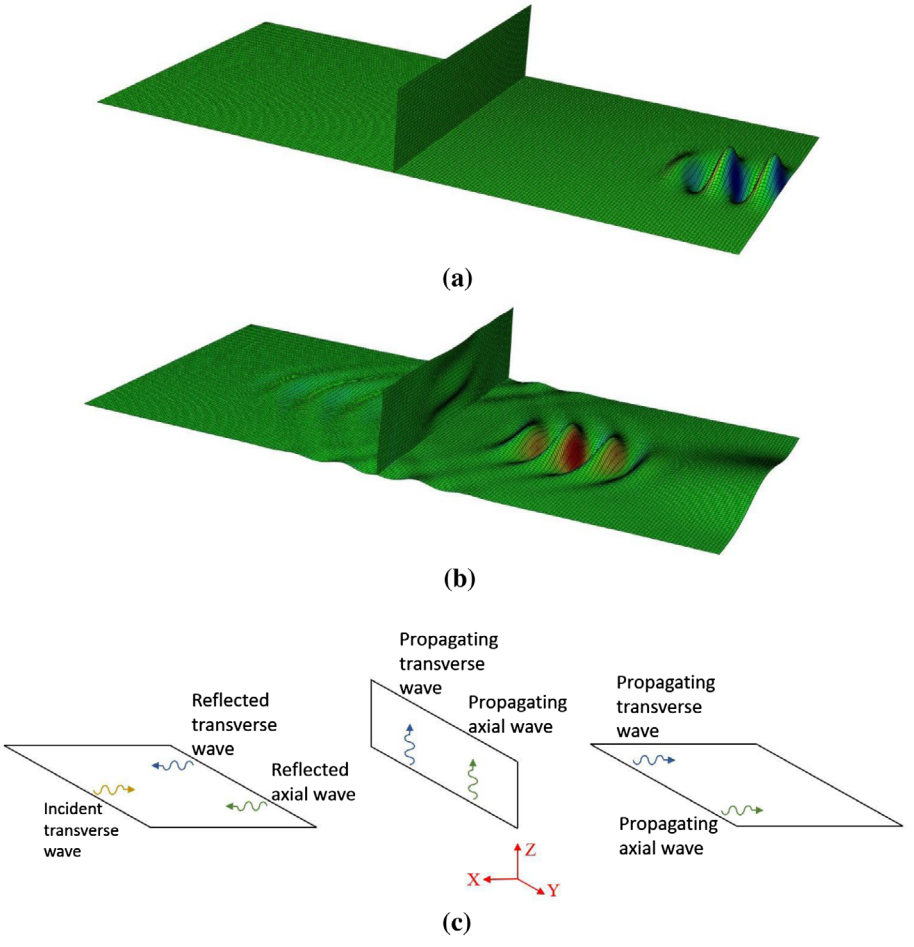

Figure 26. Wave propagation in a skin-stiffener structure at (a) 120 μs and (b) 512 μs.
Notes: Wave reflections from the stiffener are clearly observed in Figure 23(b). Figure 23(c) shows blue arrows representing waves in *Z*-direction (transverse waves) and green arrows representing waves in *X*-direction (axial waves).

Table 6. CPU time comparison – plate with stiffener.

	Number of elements	Element type	Time (sec)
UEL	3	WSFE	1117
FEM	22,500	8-noded Shell Elements	10,904

of the incident wave gets transmitted into the stiffener or the skin on the other side of the stiffener. Figure 26(c) shows the wave motion schematically, including mode conversions.

Table 6 compares run time and number of elements for FEM and UEL simulations. Again, UEL is about 10 times more efficient compared to the FEM.

5. Concluding remarks

The main objective of this research was to demonstrate the potential of integrating spectral finite element technique onto conventional finite element platform for efficient simulations of transient dynamics and wave propagation in 2-D composite structures. A wavelet spectral finite element-based user-defined element for 2-D laminated plates was formulated and implemented in a commercial finite element code (Abaqus). The WSFE is formulated in frequency domain and all of the variables and parameters are complex numbers. Since Abaqus (and other commercial finite element solvers) works only with real values, every complex number is represented as a 2×2 matrix of real numbers and then presented to Abaqus for processing. Matrix representation of complex numbers leads to doubling the number of DOFs at each node. Therefore, a spectral element with 64 spatial (Y) discretisation points at each lateral edge is modelled as 128 nodes at each lateral edge. The resulting plate element has 256 nodes with five DOFs at each node.

Five numerical examples were presented to demonstrate the ability of the newly developed element to model complex structures: healthy plate, plate with impact damage, plate with ply drop, plate with two folds and plate with stiffener. A 3.5 cycle tone-burst load with 20 kHz central frequency was used to excite the structure. For the healthy case, UEL and WSFE responses matched completely validating the UEL formulation. For all numerical examples presented, UEL and FEM (Abaqus) results compare very well, except for a few minor differences likely due to the differences in element formulations. It was shown that UEL captured the reflections from boundary, discontinuity, and damaged areas correctly. A python script was written to visualise UEL results to get a better understanding of wave propagation.

The CPU time for the UEL in all five examples is much less compared to the same simulation for FEM. For a healthy case, the CPU time for the UEL was 11% of FEM. Similar number for the other four numerical examples, namely, impact damage, ply drop, folded plate and stiffener was 32, 8, 5 and 10%, respectively. Therefore, UEL was shown to be preserving the computational efficiency of the WSFE along with the ability to model complex features using facilities available in Abaqus.

Acknowledgement

The authors would like to thank Dr. Youssef Hammi, Shahriar Sharokhabadi, Prateek Jolly and Trent Ricks of Mississippi State University for their significant help during this research.

Disclosure statement

No potential conflict of interest was reported by the authors.

References

Beskos, D. E. (1997). Boundary element methods in dynamic analysis: Part II (1986–1996). *Applied Mechanics Reviews, 50*, 149. doi:10.1115/1.3101695

Boller, C., Chang, F.-K., & Fujino, Y. (2009). *Encyclopedia of structural health monitoring*, Vol. 4. Chichester: Wiley.

Chimenti, D. E. (1997). Guided waves in plates and their use in materials characterization. *Applied Mechanics Reviews, 50*, 247. doi:10.1115/1.3101707

Dassault Systèmes Simulia Corp. 2014. *Abaqus V-6.14. User's Manual 2014.*

Daubechies, I. (1992). *Ten lectures on wavelets*, Vol. 61. Philadelphia, PA: Society for industrial and applied mathematics.

Diamanti, K., & Soutis, C. (2010). Structural health monitoring techniques for aircraft composite structures. *Progress in Aerospace Sciences, 46*, 342–352. doi:10.1016/j.paerosci.2010.05.001

Doyle, J. F. (2012). *Wave propagation in structures: Spectral analysis using fast discrete Fourier transforms*. Springer Science & Business Media.

Fornberg, B. (1987). The pseudospectral method: Comparisons with finite differences for the elastic wave equation. *Geophysics, 52*, 483–501. doi:10.1190/1.1442319

Giurgiutiu, V. (2007). *Structural health monitoring: With piezoelectric wafer active sensors*. Academic Press.

Gopalakrishnan, S., & Mitra, M. (2010). *Wavelet methods for dynamical problems*, Vol. 1, Boca Raton, FL: CRC Press/Taylor & Francis. doi:10.1201/9781439804629

Gopalakrishnan, S., Chakraborty, A., & Mahapatra, D. R. (2008). *Spectral finite element method*. London: Springer. doi:10.1007/978-1-84628-356-7

Graff, K. F. (1975). *Wave motion in elastic solids*. Courier Corporation.

Graves, R. W. (1996). Simulating seismic wave propagation in 3D elastic media using staggered-grid finite differences. *Bulletin of the Seismological Society of America, 86*, 1091–1106.

Hongbao, M. (2014). Complex number. *Natural Science, 4*, 71–78.

Khalili, A., Samaratunga, D., Jha, R., & Gopalakrishnan S. (2014). *Wavelet spectral finite element modeling of laminated composite beams with complex features*. Proceedings of the American Society for Composites 2014-Twenty-ninth Technical Conference on Composite Materials, San Diego, CA.

Khalili, A., Samaratunga, D., Jha, R., Lacy, T. E., & Gopalakrishnan S. (2015). *Wavelet spectral finite element based user-defined element in ABAQUS for modeling delamination in composite beams*. 23rd AIAA/ASME/AHS Adaptive Structures Conference, Kissimmee, FL, pp. 1–11.

Lee, B. C., & Staszewski, W. J. (2003). Modelling of Lamb waves for damage detection in metallic structures: Part I. *Smart Materials and Structures, 12*, 804–814. doi:10.1088/0964-1726/12/5/018

Lowe, M., & Pavlakovic B. (2013). *Disperse*. London: Imperial College.

Mitra, M., & Gopalakrishnan, S. (2008). Wave propagation analysis in anisotropic plate using wavelet spectral element approach. *Journal of Applied Mechanics, 75*, 014504(1)–014504(6). doi:10.1115/1.2755125

Nayfeh, A. H. (1995). *Wave propagation in layered anisotropic media: With applications to composites*. Elsevier.

Ochoa, O. O., & Reddy, J. N. (1992). *Finite element analysis of composite laminates*. Springer Science & Business Media.

Raghavan, A., & Cesnik, C. E. S. (2007). Review of Guided-wave Structural Health Monitoring. *The Shock and Vibration Digest, 39*, 91–114. doi:10.1177/058310240

Rose, J. L. (2004). *Ultrasonic waves in solid media*. Cambridge University Press.

Salahouelhadj, A., Abed-Meraim, F., Chalal, H., & Balan, T. (2012). Application of the continuum shell finite element SHB8PS to sheet forming simulation using an extended large strain anisotropic elastic-plastic formulation. *Archive of Applied Mechanics, 82*, 1269–1290. doi:10.1007/s00419-012-0620-x

Samaratunga, D., Jha, R., & Gopalakrishnan, S. (2014a). Wavelet spectral finite element for wave propagation in shear deformable laminated composite plates. *Composite Structures, 108*, 341–353. doi:10.1016/j.compstruct.2013.09.027

Samaratunga, D., Jha, R., & Gopalakrishnan, S. (2014b). Wave propagation analysis in laminated composite plates with transverse cracks using the wavelet spectral finite element method. *Finite Elements in Analysis and Design, 89*, 19–32. doi:10.1016/j.finel.2014.05.014

Samaratunga, D., Jha, R., & Gopalakrishnan, S. (2014c). Wave propagation analysis in adhesively bonded composite joints using the wavelet spectral finite element method. *Finite Elements in Analysis and Design, 89*, 19–32. doi:10.1016/j.finel.2014.05.014

Samaratunga, D., Jha, R., & Gopalakrishnan, S. (2016). Wavelet spectral finite element for modeling guided wave propagation and damage detection in stiffened composite panels. *Structural Health Monitoring, 15*, 317–334.

Strikwerda, J. C. (2004). Finite difference schemes and partial differential equations. *Society for Industrial and Applied Mathematics*, Second Edition, Pacific Grove, CA.

Su, Z., Ye, L., & Lu, Y. (2006). Guided lamb waves for identification of damage in composite structures: A review. *Journal of Sound and Vibration, 295*, 753–780. doi:10.1016/j.jsv.2006.01.020

Talbot, J. R., &, Przemieniecki, J. S. (1975). Finite element analysis of frequency spectra for elastic waveguides. *International Journal of Solids and Structures, 11*, 115–138. doi:10.1016/0020-7683(75)90106-7